Power Engineering and Engineering Thermophysics
https://www.acadlore.com/journals/PEET

Heat Absorption Performance Enhancement of TES System Using Iron Oxide/Paraffin Wax Composite

Abhishek Agarwal*

Department of Mechanical & Manufacturing Engineering Technology, Vermont State University, 05061 Vermont, USA

* Correspondence: Abhishek Agarwal (axa00275@vtc.vsc.edu)

Received: 04-03-2023 **Revised:** 05-05-2023 **Accepted:** 05-13-2023

Citation: A. Agarwal, "Heat absorption performance enhancement of TES system using iron oxide/paraffin wax composite," *Power Eng. Eng. Thermophys.*, vol. 2, no. 2, pp. 73–85, 2023. https://doi.org/10.56578/peet020202.

Abstract: Thermal Energy Storage (TES) system has emerged as a promising solution of energy demand and supply management, which stores excess thermal energy and releases it when energy demand is high, making it an efficient and cost-effective energy storage solution when combined with renewable energy sources, such as solar and wind power. This study aimed to evaluate the thermal performance of TES units using Computational Fluid Dynamics (CFD) simulations in the ANSYS CFX software package. After comparing the heat storage capacity of conventional Phase Change Material (PCM) and iron oxide/paraffin wax composite (2%) using industrial residual water, temperature distribution plots and heat flux data were generated in simulations for both cases. Addition of iron oxide nanoparticles significantly improved the heat absorption performance of TES units. Both materials initially exhibited a higher heat absorption rate, which gradually decreased over time. CFD data analysis revealed that iron oxide/paraffin wax material enhanced heat absorption performance by up to 1.3%, which demonstrated the potential of iron oxide nanoparticles in improving the efficiency of TES system and highlighted the advantages of TES system combined with renewable energy sources. By improving heat absorption properties, the incorporation of iron oxide nanoparticles had the potential to increase the lifespan of TES units and significantly reduced maintenance and replacement expenses. This breakthrough, along with the cost savings and energy efficiency offered by TES technology, may encourage its widespread application, thus reducing reliance on fossil fuels and promoting sustainable energy practices.

Keywords: Thermal energy storage (TES); Renewable energy sources; Iron oxide nanoparticles; Heat absorption performance; Computational fluid dynamics; Phase change materials

1 Introduction

TES system has become increasingly popular in recent years, driven by the growing demand for sustainable energy solutions. It is particularly useful in areas with fluctuating energy supply and demand, and with the need to store excess thermal energy of renewable energy sources [1]. TES system has different types, with each having its own advantages and disadvantages. The most commonly used type is sensible heat storage, which heats or cools a storage medium, such as water or rocks, to store thermal energy, and is reliable, easy to maintain, and cost-effective. Another TES system type is latent heat storage, which stores thermal energy by changing the phase of the storage medium, such as changing a solid to a liquid. The latent heat storage system stores more energy, though it is more complex and expensive than the sensible heat storage. Thermochemical storage system is also a TES system type, which stores thermal energy using a chemical reaction to absorb or release heat. It stores a large amount of energy and has a high energy density, but is still in the early development stage and not widely used. Figure 1 illustrates a typical TES system, which stores thermal energy by heating or cooling a storage medium, such as water or molten salts, to maintain a constant temperature within the system.

With the increasing demand for sustainable energy solutions, TES system is expected to play more important role in meeting the global energy needs. In addition, it can be used in combination with other energy storage technologies, such as batteries or flywheels, to provide a complete energy storage solution. Overall, TES system has the potential to revolutionize energy storage and use, because it offers a reliable and cost-effective way to store thermal energy of

renewable energy sources and helps reduce the reliance on fossil fuels. As the research into TES system continues, it is expected to see even more innovative applications in the years to come.

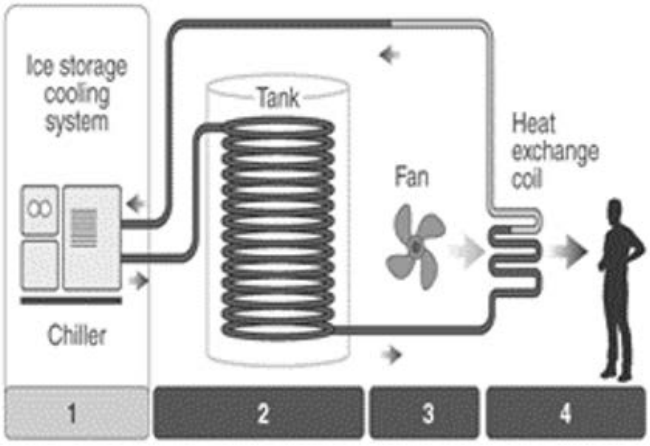

Figure 1. TES system [2]

Rahman et al. [3] emphasized the vital role of energy storage system in optimizing the use of renewable energy sources, and focused on TES system among various storage technologies analyzed. Advantages and limitations of the system were presented, and its potential for enhancing energy efficiency and promoting sustainable energy practices was highlighted. The importance of TES technology was illustrated, which contributed significantly to the discourse on sustainable energy and its vital role in shaping a greener future. Furthermore, the study was valuable for researchers and practitioners seeking to explore the possibilities of TES system for renewable energy applications. Tawalbeh et al. [4] simulated CFD to investigate the performance of a hybrid photovoltaic/solar chimney seawater desalination plant located in the United Arab Emirates. The findings demonstrated that the plant produced fresh water at lower costs than traditional desalination plants. Furthermore, the study showed that incorporation of TES significantly increased the plant's efficiency and reliability. In a related review, Hussain et al. [5] comprehensively outlined various energy storage technologies, including TES system. In addition, the study discussed the different TES system types and their respective advantages and limitations, and highlighted their potential applications in areas, such as building heating and cooling, industrial processes, and renewable energy systems.

In a comprehensive review of latent TES technologies, Jouhara et al. [6] delved into different PCMs used in TES system, and highlighted their advantages and limitations. In addition, the potential applications of these technologies in various industries were explored, including renewable energy and industrial processes. The study provided a wealth of information for researchers and practitioners seeking to understand the possibilities of the TES system. Dogkas et al. [7] investigated the potential of utilizing paraffin as PCM in a TES unit for cooling applications in buildings. The study revealed that the system efficiently stored thermal energy and released it as needed. Staggered heat exchanger also allowed for less than 10 kW of heat transfer when the water outlet temperature ranged between 5°C and 10°C, which was easily provided by a typical commercial heat pump. The results provided valuable insights into the effectiveness of paraffin as PCM in the TES system. Overall, the study highlighted the potential of paraffin as a viable option for TES in cooling applications. Okogeri and Stathopoulos [8] reviewed biobased PCMs for TES applications. The advantages and limitations of various biobased PCMs were discussed, and their potential as a sustainable and environmentally friendly alternative to conventional PCM was highlighted. Calati et al. [9] reviewed PCM-based thermal storage for refrigerated transport and distribution applications along the cold chain. The challenges of maintaining quality and safety of temperature-sensitive products during transportation and storage were discussed, and the potential of PCM-based TES system to address these challenges was highlighted.

Rimpel et al. [10] provided an overview of mechanical energy storage technologies, including flywheels, compressed air energy storage, and pumped hydro storage. Advantages and limitations of these technologies were discussed, and their potential of being used in large-scale energy storage applications was highlighted. Tawalbeh et al. [11] classified various TES materials, including sensible heat storage materials, latent heat storage materials, and thermochemical storage materials. Advantages and limitations of various types of materials were discussed, and their potential of being used in various applications was highlighted, such as building heating and cooling, industrial processes, and renewable energy systems. Miller et al. [12] provided an overview of chemical energy storage technologies, including hydrogen storage, redox flow batteries, and fuel cells. Advantages and limitations of these technologies were discussed, and their potential of being used in large-scale energy storage applications

was highlighted. Aneke and Wang [13] reviewed energy storage technologies and their real-life applications. The importance of energy storage systems for efficient utilization of renewable energy sources was discussed, and examples of various energy storage technologies and their applications in the electricity grid, transportation, and buildings were provided.

In recent years, TES system has become a promising solution for efficient and sustainable energy practices. However, TES units are heavily reliant on the heat absorption performance of their storage materials. Therefore, it is crucial to choose suitable materials with desired thermal storage properties in order to obtain efficient results in sensible heat storage technology. The storage material should have high thermal storage capacity, adequate thermal conductivity, excellent packing factor, high toughness, compressive strength, stability, low self-discharge and thermal expansion, and be low-cost, non-toxic, non-explosive, non-flammable, non-corrosive, and environmentally friendly. To address this issue, this study aimed to evaluate the thermal performance of TES units utilizing CFD, under the hypothesis that iron oxide/paraffin wax composite material enhanced the heat absorption performance of TES system compared with conventional paraffin wax material. By comparing the heat storage capacity of iron oxide/paraffin wax composite material and conventional paraffin wax material in TES units, and studying temperature distribution plots and heat flux data for both cases, this study provided critical insights into the effectiveness of the iron oxide/paraffin wax composite material in enhancing the heat absorption performance of TES system.

2 Methodology

CFD simulation process for TES units included three stages: preprocessing, solution, and post-processing. In the preprocessing stage, a computer-aided design (CAD) model of the TES units was created, the computational domain was meshed, and thermal boundary conditions and solver settings were defined. Then the software proceeded to the solution stage, carried out multiple iterations and determined Root Mean Square (RMS) residual values of mass, momentum, and energy at each iteration. Finally, contour plots of temperature distribution and heat flux across the TES units were generated in the post-processing stage, providing a visual representation of the simulation data. This rigorous simulation process provided critical insights into the thermal performance of TES units and allowed for the evaluation of different materials and configurations. By accurately modeling and analyzing the performance of TES units, researchers and engineers made informed decisions and optimized the crucial energy storage system design [14]. The shell and tube design of TES units was modeled using Creo Parametric software, based on the guidelines in the study of Sun et al. [15]. The thermal performance of TES units was analyzed, utilizing CFDgenerated temperature distribution plots and heat flux data. The heat storage capacity of the conventional paraffin wax material and the iron oxide/paraffin wax composite material was compared, and the effectiveness of the latter in heat absorption performance enhancement of TES units was evaluated. Table 1 shows the shell and tube dimensions of TES units.

Table 1. Dimensions of shell and tube in TES units [15]

Item	Symbol	Value	Unit
Tube length	L	3000	mm
Internal radius of interior tube	r_i	26	mm
External radius of interior tube	r_o	30	mm

The CFD analysis of TES units comprised of two different materials, paraffin wax and iron oxide/paraffin wax. The study of Jebali et al. [16] demonstrated that the inclusion of nanoparticles in paraffin wax enhanced the thermal conductivity. Paraffin wax had only 0.259 W/m-K of thermal conductivity, while the thermal conductivity of paraffin wax/iron oxide increased to 0.298 W/m-K, which was especially advantageous for TES units, because it enabled the PCM to extract heat from industrial residual water at a quicker rate. Use of iron oxide nanoparticles significantly increased the effectiveness of TES units, leading to greater energy savings and the promotion of more sustainable energy practices. Figure 2 displays the CAD model of the shell and tube structure in TES units, showcasing the innovative design of this study.

Taking into account the geometry type and topological consistency of TES units, the model was carefully discretized to ensure optimal accuracy in the analysis [17–20]. A fine relevance approach was utilized in the meshing process (Figure 3), ensuring that the model was adequately represented in the CFD analysis. A total of 87,949 elements and 120,391 nodes were generated in the meshing process, providing a comprehensive and detailed representation of TES units. The rigorous modeling process maintained the topological consistency of TES units, making it suitable for brick/hexahedral element type. This approach allowed for a detailed thermal performance assessment of TES units, providing valuable insights into the heat absorption performance enhancement and effectiveness.

After the meshing, the computational domain of TES system was defined (Figure 4) and segmented based on the present material type.

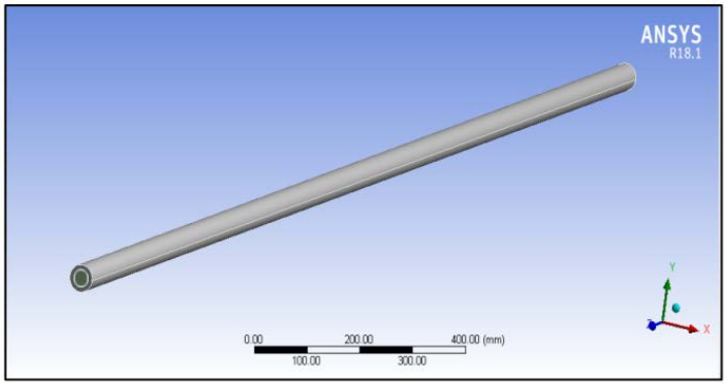

Figure 2. CAD model of shell and tube structure

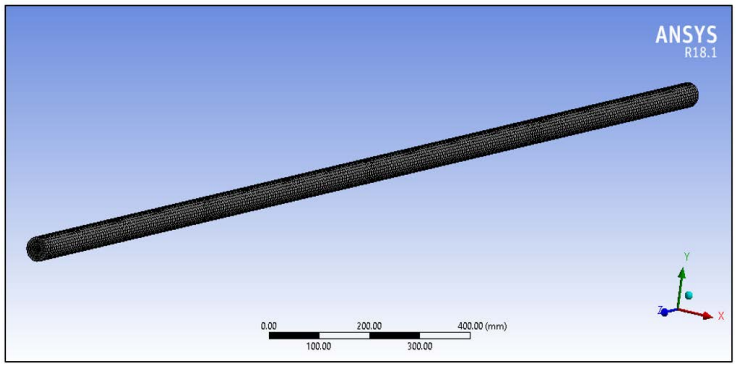

Figure 3. Meshed model of shell and tube structure

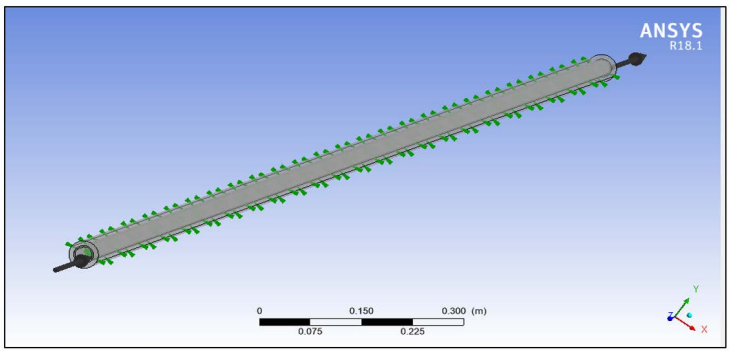

Figure 4. Domain definition of shell and tube structure

Three distinct domains were defined for this analysis, namely, industrial water, copper tube, and PCM, which involved specifying material properties, reference pressure, and turbulence model. Material properties for both paraffin wax and iron oxide/paraffin wax were defined to ensure precise and accurate simulations. The defined computational domain and material properties helped generate accurate temperature distribution plots and heat flux data, which were used to evaluate the effectiveness of TES units as given in Table 2.

Table 2. Material definition

Material type	**Density** $\left(\mathbf{gm/cm^3}\right)$	**Thermal conductivity (W/m-K)**
Paraffin wax	0.95	0.259
Iron oxide with paraffin wax	1.2	0.298

The TES system included inner domain, through which industrial residue water flowed (Figure 5). In this process, the domain was defined, including material definition and reference pressure (1atm).

Then the paraffin wax domain (Figure 6) was defined as solid type, with thermal energy as the energy model.

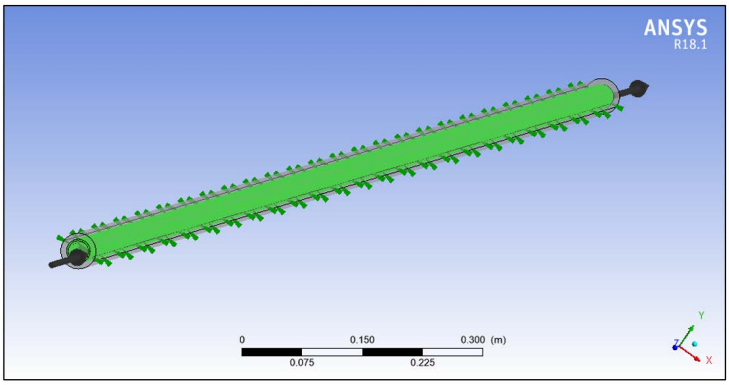

Figure 5. Residual water domain

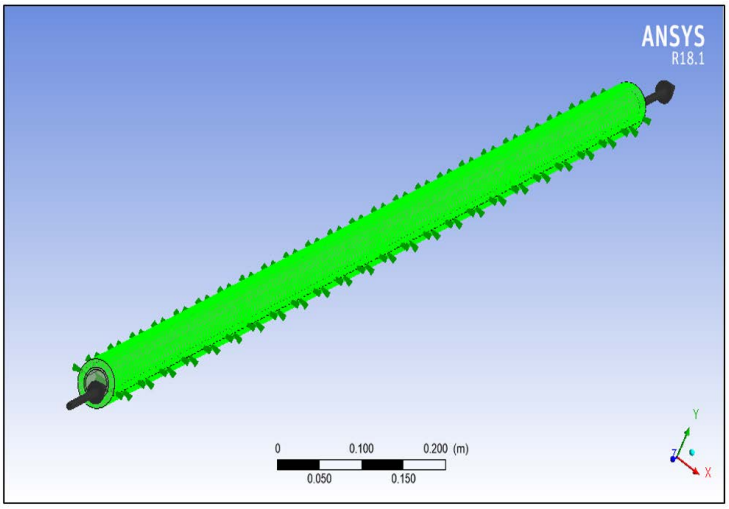

Figure 6. Paraffin wax domain

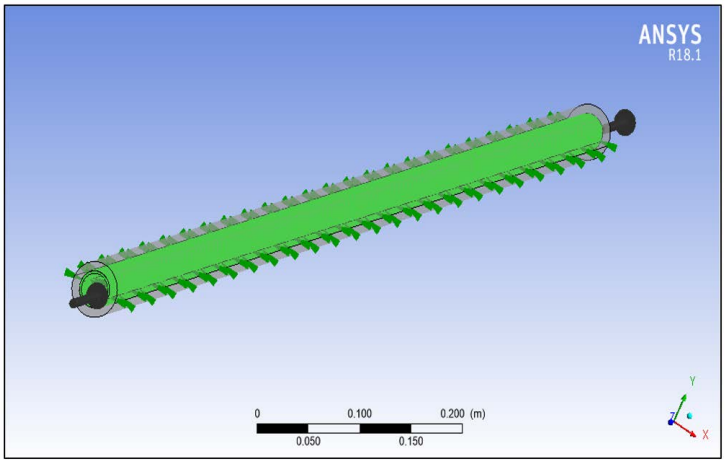

Figure 7. Copper domain

The copper domain (Figure 7) was between outer paraffin wax domain and inner residual water domain and defined as solid type, with thermal energy as the heat transfer model. Then the inlet and outlet boundary conditions were defined for residual water from Figure 8 to Figure 11.

Water inlet boundary condition included definition of 0.278 Kg/s mass flow rate and 70℃ temperature [15]. Residual water outlet was also defined for TES units as shown in Figure 10, including 0Pa relative pressure difference and 0.05 pressure profile blend, as shown in Figure 11.

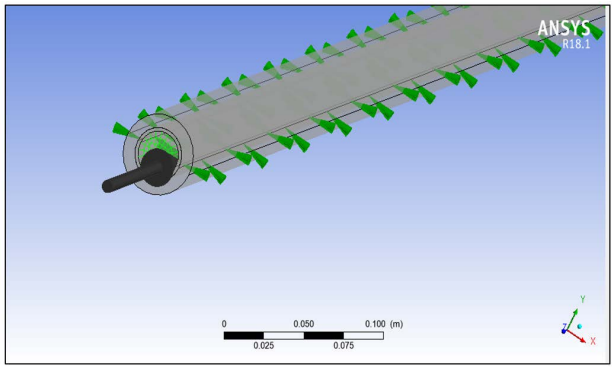

Figure 8. Residual water inlet boundary

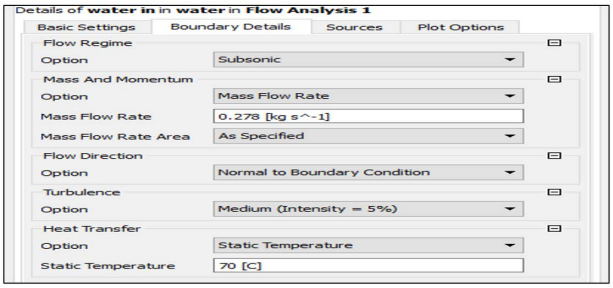

Figure 9. Defining water inlet boundary

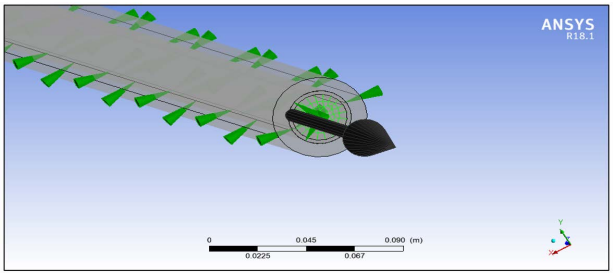

Figure 10. Residual water outlet boundary

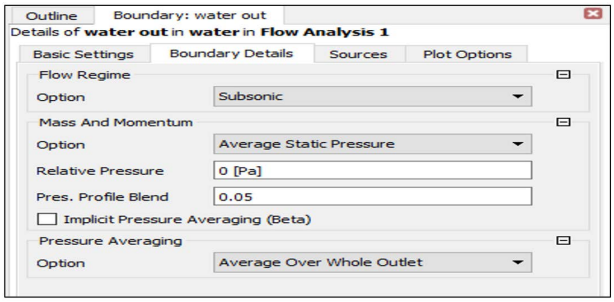

Figure 11. Water outlet boundary values

Transient settings were defined for the simulation, including total time (500 secs) and time steps (25 secs). The simulation began after defining the water outlet boundary condition. The solver settings included 0.00001 RMS residual target, and upwind type interpolation scheme.

3 Results and Discussion

CFD simulation generated temperature distribution plots at various time steps for two different PCMs: paraffin wax and iron oxide/paraffin wax. This analysis provided detailed insights into the thermal performance of TES units, and highlighted the benefits of innovative iron oxide/paraffin wax composite material. CFD simulation provided a detailed understanding of temperature distribution within the TES units and valuable data to assess the effectiveness of different PCMs in heat absorption performance enhancement of the system. Comparison of the two PCMs provided a valuable insight into the potential benefits of iron oxide/paraffin wax composite material in TES units, and highlighted its superior heat absorption capabilities.

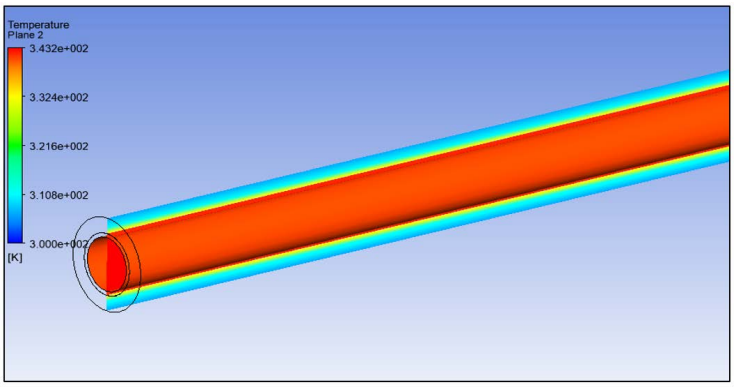

Figure 12. Temperature plot at 100 secs using paraffin wax

The temperature distribution plot of TES units at 100 secs using paraffin wax was generated after simulation, as shown in Figure 12. The temperature was 332K near the copper zone, which was higher, and 310K in the outer region of paraffin wax, which was lower.

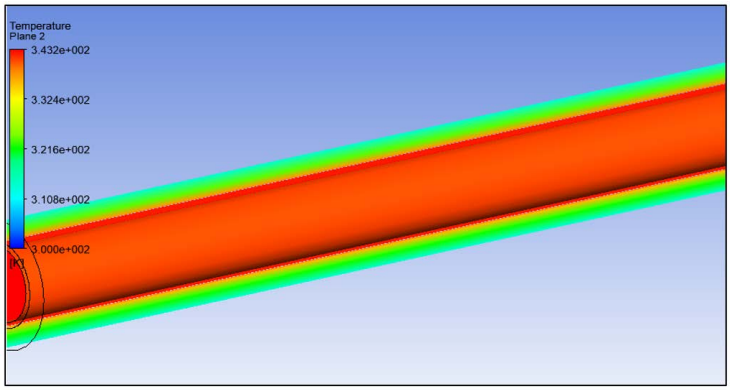

Figure 13. Temperature plot at 200 secs using paraffin wax

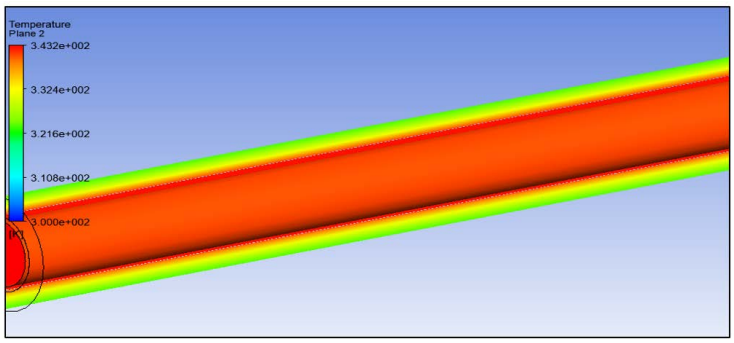

Figure 14. Temperature plot at 300 secs using paraffin wax

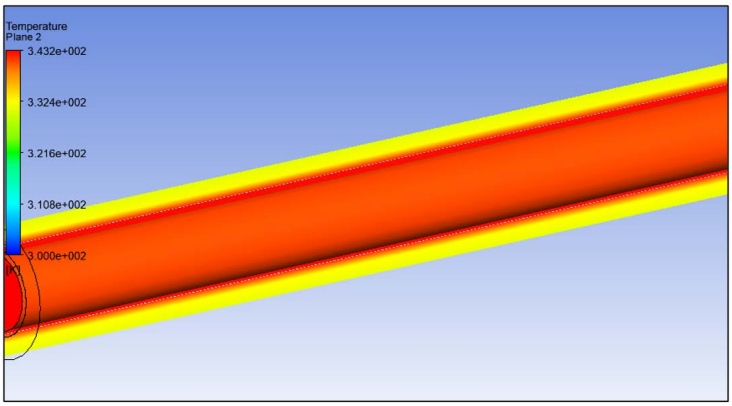

Figure 15. Temperature plot at 400 secs using paraffin wax

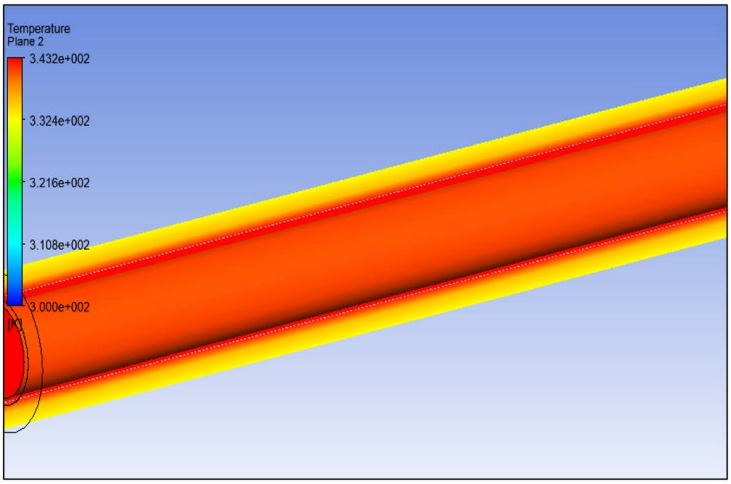

Figure 16. Temperature plot at 500 secs using paraffin wax

The temperature distribution plot of TES units at 200 secs using paraffin wax was generated after simulation, as shown in Figure 13. The temperature was 332K near the copper zone and 321K in the outer region of paraffin wax. Similarly, temperature distribution plots at 300 secs, 400 secs and 500 secs were obtained, as shown in Figure 14, Figure 15 and Figure 16.

Figure 16 displays the temperature distribution plot of TES units at 500 secs using paraffin wax obtained from the simulation. The plot clearly visualized the temperature distribution within TES units, showing that the temperature near the copper zone reached 343K, which was considerably higher, while the outer region of paraffin wax had a lower temperature of 335.2K.

Table 3. Grid independence test

Number of elements	Residual water temp (K)
87,958	334.8
98,995	334.9
10,155	335.1
10,171	335.2
10,186	335.2

To ensure the accuracy of the simulation results, a grid independence test was performed on the TES units. Temperature was measured at a specific point and the results are shown in Table 3. The temperature at this point was 335.2K, which was closely consistent with the temperature obtained from experimental data (337K) [15], which highlighted the reliability and accuracy of the CFD simulation results. Further analysis of TES units was made using iron oxide/paraffin wax composite. The thermo-physical properties of iron oxide/paraffin wax were taken from the study of Jebali et al. [16].

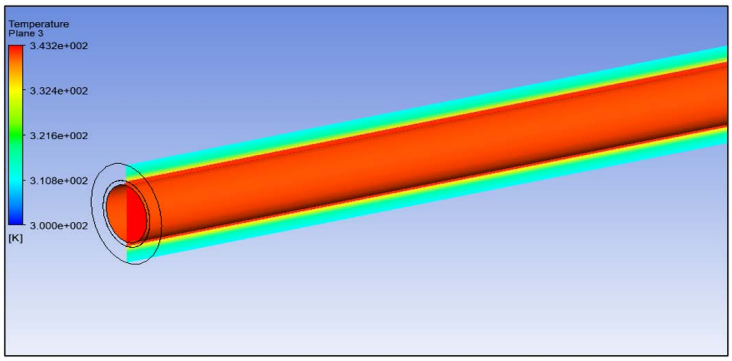

Figure 17. Temperature plot at 100 secs using paraffin wax/iron oxide

The temperature distribution plot of TES units at 100 secs using paraffin wax/iron oxide composite was generated after simulation and is shown in Figure 17. The temperature in the outer region of paraffin wax/iron oxide was 318K.

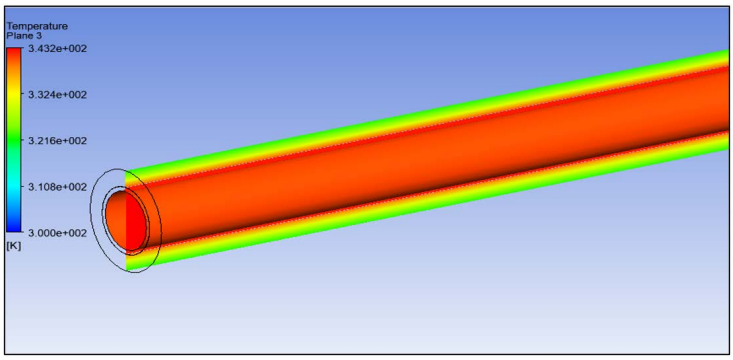

Figure 18. Temperature plot at 200 secs using paraffin wax/iron oxide

The temperature distribution plot of TES units at 200 secs using paraffin wax/iron oxide composite was generated after simulation and is shown in Figure 18. The temperature in the outer region of paraffin wax/iron oxide was 321K.

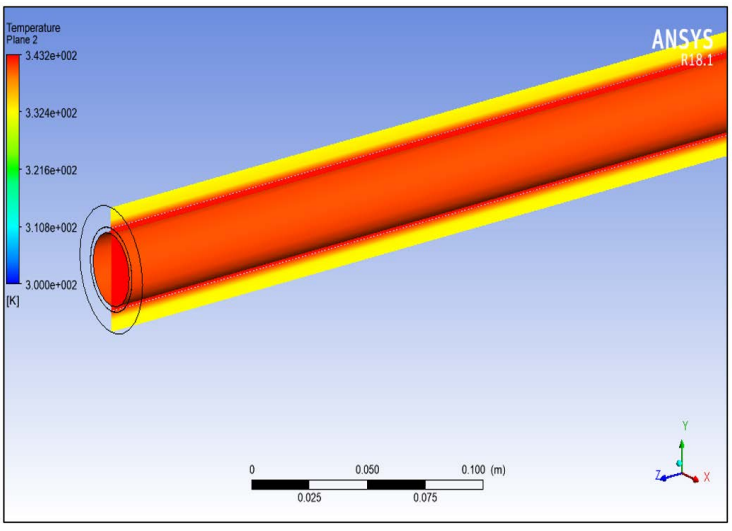

Figure 19. Temperature plot at 300 secs using paraffin wax/iron oxide

The temperature distribution plot of TES units at 300 secs using paraffin wax/iron oxide composite was generated after simulation and is shown in Figure 19. The temperature in the outer region of paraffin wax/iron oxide was 332K.

The temperature distribution plot of TES units at 400 secs using paraffin wax/iron oxide composite was generated after simulation and is shown in Figure 20. The temperature in the outer region of paraffin wax/iron oxide was 338K.

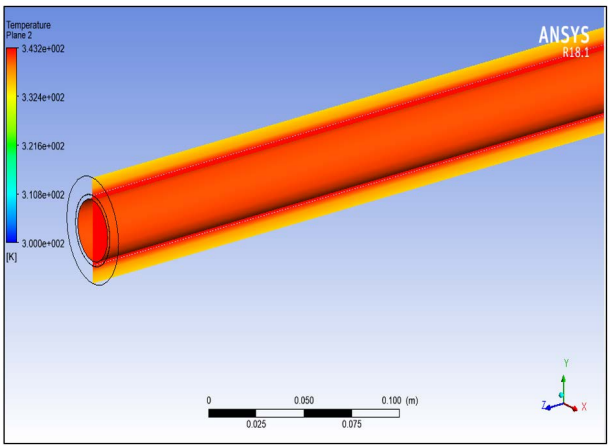

Figure 20. Temperature plot at 400 secs using paraffin wax/iron oxide

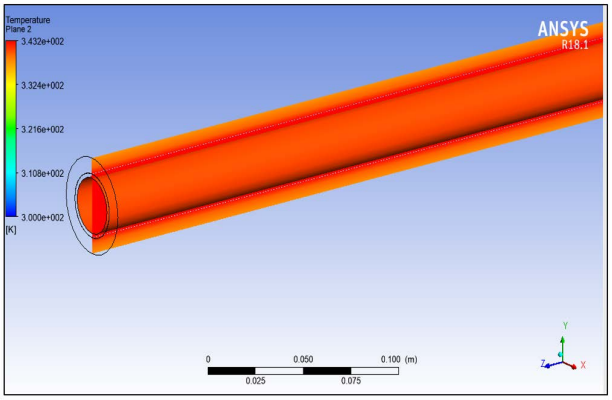

Figure 21. Temperature plot at 500 secs using paraffin wax/iron oxide

Table 4. Temperature and time data for use of paraffin wax only

Time [s]	Temperature [K]
0.00	300.00
25.00	302.05
50.00	305.12
75.00	308.47
100.00	311.73
125.00	314.73
150.00	317.44
175.00	319.87
200.00	322.03
225.00	323.97
250.00	325.70
275.00	327.26
300.00	328.67
325.00	329.94
350.00	331.10
375.00	332.15
400.00	333.11
425.00	333.98
450.00	334.77
475.00	335.50
500.00	336.16

The temperature distribution plot of TES units at 500 secs using paraffin wax/iron oxide composite was generated after simulation and is shown in Figure 21. The temperature in the outer region of paraffin wax/iron oxide was 340K. Table 4 shows the temperature and time data for use of paraffin wax only.

Table 5 summarizes the temperature and time data for use of paraffin wax with 2% iron oxide.

Table 5. Temperature and time data for use of paraffin wax with iron oxide 2% only

Time [s]	Temperature [K]
0.00	300.00
25.00	303.38
50.00	307.93
75.00	312.45
100.00	316.50
125.00	320.00
150.00	323.00
175.00	325.56
200.00	327.77
225.00	329.69
250.00	331.35
275.00	332.80
300.00	334.06
325.00	335.17
350.00	336.14
375.00	336.99
400.00	337.74
425.00	338.40
450.00	338.98
475.00	339.49
500.00	339.93

The heat absorption performance of both materials was evaluated, paraffin wax only and paraffin wax with 2% iron oxide particles. The heat absorption of PCM was given by $Q = q^* A$.
where, q is the heat flux $(\mathrm{W}/\mathrm{m}^2)$ determined by the functional calculator of ANSYS CFX simulation package, A is the area (m^2) of annulus. The cross-sectional area of exposed surface was 0.282 m^2, which was determined by Creo design software.

Table 6. Heat absorption comparison table

Time (s)	Heat absorbed by paraffin wax (W)	Heat absorbed by paraffin wax/iron oxide (W)
25	782.78	795.27
50	707.88	712.54
75	621.33	629.41
100	548.21	551.69
125	485.80	489.74
150	432.98	437.24
175	387.97	391.25
200	355.31	363.4
225	320.74	323.15

Based on the data, the heat absorption performance was evaluated and is shown in Table 6. The simulation results showed that the maximum heat absorption value occurred at the initial 25 secs of the simulation, with 782.7W for paraffin wax and 795.27W for paraffin wax/iron oxide. As shown in the above table, the heat absorption value of paraffin wax/iron oxide was always higher than that of paraffin wax throughout the simulation, which indicated that the addition of iron oxide nanoparticles to paraffin wax significantly enhanced the heat absorption performance. The heat absorption improvement in TES units has significant practical implications. TES system is widely used to store thermal energy for later use in heating and cooling applications. Efficiency improvement of the heat absorption process optimizes the overall performance of TES units, leading to reduced energy costs and improved sustainability. Therefore, the results of this study have important implications for developing more efficient and effective TES system, thus significantly promoting the use of sustainable energy sources.

4 Conclusion

The CFD tool was utilized to evaluate the heat transfer performance of a new PCM, paraffin wax with iron oxide nanoparticles, in TES units. It was found that the incorporation of iron oxide nanoparticles enhanced the heat absorption performance of TES units, with the maximum improvement of 1.3% compared with pure paraffin wax. This improvement can be translated into real-world applications, such as efficiency improvement of TES system and reduction of energy costs. The addition of iron oxide nanoparticles increased the energy storage capacity of TES units, which was an attractive solution for applications requiring long-term TES. Furthermore, iron oxide nanoparticles helped reduce energy losses within the TES units by minimizing thermal gradients and enhancing heat transfer, which improved overall efficiency, reduced maintenance costs, and potentially increased the lifespan of TES units. Wider application of TES technology can lead to reduced reliance on fossil fuels and more sustainable energy practices, making it an attractive option for policymakers and industry leaders.

Compared with pure paraffin wax, the heat absorption performance of paraffin wax with iron oxide nanoparticles increased by 1.59%, 1.32%, 0.63% and 0.84% after 25 secs, 75 secs, 100 secs and 175 secs of the simulation, respectively, which were the key findings of the study.

Overall, this study highlighted the potential of iron oxide nanoparticles in optimizing the TES system efficiency and provided a promising direction for developing sustainable energy storage solutions. The findings of this study have significant implications for the energy industry and policymakers, paving the way for more sustainable energy practices.

Data Availability

The data used to support the findings of this study are available from the corresponding author upon request.

Conflicts of Interest

The authors declare that they have no conflicts of interest.

References

[1] A. Agarwal, O. B. Molwane, and I. Pitso, "Thermal analysis & modelling of phase change material used in low temperature industrial wastewater applications," *Mater. Today: Proc.*, vol. 39, pp. 596–605, 2021. https://doi.org/10.1016/j.matpr.2020.08.612

[2] "How thermal energy storage works," https://www.calmac.com/how-energy-storage-works, 2022.

[3] M. M. Rahman, A. O. Oni, E. Gemechu, and A. Kumar, "Assessment of energy storage technologies: A review," *Energy Convers. Manage.*, vol. 223, p. 113295, 2020. https://doi.org/10.1016/j.enconman.2020.113295

[4] M. Tawalbeh, S. Mohammed, A. Alnaqbi, S. Alshehhi, and A. Al-Othman, "Analysis for hybrid photovoltaic/solar chimney seawater desalination plant: A CFD simulation in Sharjah, United Arab Emirates," *Renew. Energy*, vol. 202, pp. 667–685, 2023. https://doi.org/10.1016/j.renene.2022.11.106

[5] F. Hussain, M. Z. Rahman, A. N. Sivasengaran, and M. Hasanuzzaman, "Energy storage technologies," *Energy Sustain. Dev.*, pp. 125–165, 2020. https://doi.org/10.1016/B978-0-12-814645-3.00006-7

[6] H. Jouhara, A. Żabnieńska Góra, N. Khordehgah, D. Ahmad, and T. Lipinski, "Latent thermal energy storage technologies and applications: A review," *Int. J. Thermofluids*, vol. 5, p. 100039, 2020. https://doi.org/10.1016/j.ijft.2020.100039

[7] G. Dogkas, M. K. Koukou, J. Konstantaras, C. Pagkalos, K. Lymperis, V. Stathopoulos, L. Coelho, A. Rebola, and M. G. Vrachopoulos, "Investigating the performance of a thermal energy storage unit with paraffin as phase change material, targeting buildings' cooling needs: An experimental approach," *Int. J. Thermofluids*, vol. 3, p. 100027, 2020. https://doi.org/10.1016/j.ijft.2020.100027

[8] O. Okogeri and V. N. Stathopoulos, "What about greener phase change materials? A review on biobased phase change materials for thermal energy storage applications," *Int. J. Thermofluids*, vol. 10, p. 100081, 2021. https://doi.org/10.1016/j.ijft.2021.100081

[9] M. Calati, K. Hooman, and S. Mancin, "Thermal storage based on phase change materials (PCMs) for refrigerated transport and distribution applications along the cold chain: A review," *Int. J. Thermofluids*, p. 100224, 2022. https://doi.org/10.1016/j.ijft.2022.100224

[10] A. Rimpel, K. Krueger, Z. Y. Wang, and et al., "Mechanical energy storage," *Thermal, Mechanical, and Hybrid Chemical Energy Storage Systems*, pp. 139–247, 2021. https://doi.org/10.1016/B978-0-12-819892-6.00004-6

[11] M. Tawalbeh, A. Al-Othman, N. Ashoobi, and M. Alkasrawi, "Classifications of thermal energy storage materials," *Encyclopedia of Smart Materials*, 2022. http://dx.doi.org/10.1016/B978-0-12-815732-9.00064-4

[12] M. A. Miller, J. Petrasch, K. Randhir, N. Rahmatian, and J. Klausner, "Chemical energy storage," *Int. J. Thermofluids*, 2020. https://doi.org/10.1016/B978-0-12-819892-6.00005-8

[13] M. Aneke and M. Wang, "Energy storage technologies and real life applications–A state of the art review," *Appl. Energy*, vol. 179, pp. 350–377, 2016. https://doi.org/10.1016/j.apenergy.2016.06.097

[14] A. Agarwal, O. B. Molwane, and I. Pitso, "Analytical investigation of the influence of natural gas leakage and safety zone in a pipeline flow," *Mater. Today, Proc.*, vol. 39, pp. 547–552, 2021. https://doi.org/10.1016/j.matpr.2020.08.335

[15] W. Sun, Z. Zhao, and Y. Wang, "Thermal analysis of a thermal energy storage unit to enhance aworkshop heating system driven by industrial residual water," *Energies*, vol. 10, no. 2, 2017. https://doi.org/10.3390/en10020219

[16] M. Jebali, G. Colangelo, L. Haurie, I. Bekri-Abbes, and A. M. Lacasta, "Thermo-physical properties of paraffin wax with iron oxide nanoparticles as phase change material for heat storage applications," *J. Phys.: Conf. Ser.*, vol. 2385, no. 1, p. 012026, 2022. https://doi.org/10.1088/1742-6596/2385/1/012026

[17] A. Agarwal, "Computational investigation of vertical axis wind turbine in hydrogen gas generation using PEM electrolysis," *J. New Mater. Electrochem. Syst.*, vol. 25, no. 3, pp. 172–178, 2022. http://dx.doi.org/10.14447/jnmes.v25i3.a03

[18] A. Agarwal and M. T. Letsatsi, "Heat transfer characteristics of flame jet impingement with methane air reaction environment," *Mater. Today: Proc.*, vol. 39, pp. 789–795, 2021. https://doi.org/10.1016/j.matpr.2020.09.635

[19] A. Agarwal and M. T. Letsatsi, "Investigation of the effect of engine cylinder fin shape on heat transfer characteristics under forced convection," *Emerging Trends in Mechanical and Industrial Engineering*, pp. 113–128, 2023. https://doi.org/10.1007/978-981-19-6945-4_9

[20] A. Agarwal and M. T. Letsatsi, "FSI investigation of cooling tower subjected to high gusts," *Mater. Today: Proc.*, vol. 60, pp. 2141–2150, 2022. https://doi.org/10.1016/j.matpr.2022.02.060